JOURNAL OF MATERIALS SCIENCE 26 (1991) 2133 - 2136

Isothermal crystallization kinetics of the $Ni_{63}Cr_{18}Si_{13}B_6$ alloy

M. MILLÁN, A. CONDE
Departamento de Física de la Materia Condensada, Instituto de Ciencias de Materiales, Universidad de Sevilla-C.S.I.C., Apartado 1065, 41080 Sevilla, Spain

Isothermal crystallization kinetics of the $Ni_{63}Cr_{18}B_{13}Si_6$ alloy was carried out by differential scanning calorimetry. The JMA approach was used and the mean Avrami exponent values obtained were found to be consistent with a primary precipitation and a polymorphic crystallization, respectively, for the two crystallization stages. The novel concept of the local value of the Avrami exponent was also applied. The $n_{loc}-x$ plot was seen to be independent of the temperature of isothermal crystallization for the two stages, indicating that the crystallization processes depend only on the volume fraction transformed. Finally, the time-scaling law in the kinetic plots was verified.

1. Introduction

Metallic glasses prepared by rapid solidification techniques are thermodynamically unstable and relax towards a more stable condition during thermal annealing which finally leads to crystallization. An understanding of the crystallization processes in metallic glasses is of prime technological importance because many physical properties of these glasses are altered significantly on crystallization [1, 2]. Thermal analysis techniques such as differential scanning calorimetry (DSC) provide convenient methods for obtaining information on the transformation kinetics.

The Johnson–Mehl–Avrami equation has been used extensively to analyse the crystallization kinetics of a wide range of metallic systems. For isothermal crystallization, a linear fit of $\ln[-\ln(1-x)]$ against $\ln t$, where x is the volume fraction transformed in time t, provides the Avrami exponent. Calka and Radlinski [3] have shown that the calculation, as usual, of a mean value of the Avrami exponent over a range of crystallized fractions may be inappropriate if competing reactions or changes in growth dimensions occur during the transformation. Although most of the published work on the crystallization of metallic glasses reports correlation coefficients of 0.99 or better in the linear fit of the Avrami plots, some deviation from the linearity over the full range of volume fraction transformed can be detected [4, 5]. A more sensitive approach is to plot the first derivative of the Avrami plot against the volume fraction transformed [3, 6], which gives the local value of the Avrami index with the crystallized fraction. Such a plot allows the detection of changes in reaction kinetics during the progress of the crystallization.

In this paper, the technique suggested by Calka and Radlinski is applied to a nickel-based metallic glass, and a time-scaling law is applied to the kinetic plots. Early work on this material, including constant heating rate DSC experiments and X-ray diffraction characterization of crystalline phases, was recently reported [7].

2. Experimental procedure

Amorphous ribbons 25 mm wide and 30 μm thick with nominal composition $Ni_{63}Cr_{18}B_{13}Si_6$ were kindly supplied by Allied Chemicals Co. DSC experiments were carried out in a Perkin–Elmer DSC-2C calorimeter. Both temperature and energy calibrations were checked using lead and K_2SO_4 standards. For isothermal runs, pieces of the samples about 5 mg in weight, were heated to the annealing temperature at the maximum available rate (320 K min^{-1}) from room temperature to prevent unwanted annealing. All the DSC work was carried out in a flowing argon atmosphere.

The ordinate in the DSC scans is proportional to the net power input to the sample, relative to the power input to a stable reference sample. The instantaneous rate of change in the volume fraction of transformed material is

$$dx/dt = (1/\Delta H)dq/dt \quad (1)$$

where dq/dt is the power, ΔH is the enthalpy of the transformation and it is assumed that the heat per gram of the transformation is uniform in time. ΔH is obtained from the total area between the transformation curve and a properly constructed baseline. Integration of the experimental isothermal DSC curve from $t = 0$ at the start of the transformation to any later time yields the volume fraction $x(t)$ as the ratio of the corresponding partial area β, measured in the same units as the total area α, such that $\beta = \alpha x$, because $x = 1$ at completion. Thus the DSC record yields partial area to the total area β/α. The peak areas were measured with an image analyser.

0022–2461/90 $03.00 + .12

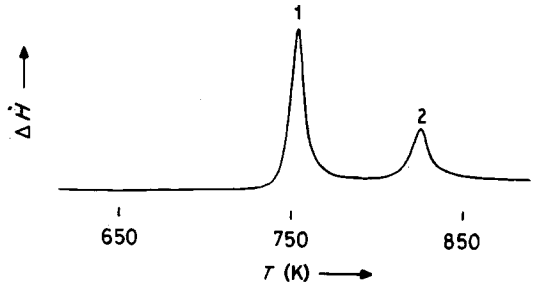

Figure 1 DSC record at 20 K min^{-1}.

3. Results and discussion

The crystallization behaviour of the $Ni_{63}Cr_{18}B_{13}Si_6$ alloy has recently been investigated by continuous heating DSC and X-ray diffraction [7]. A DSC record of the amorphous ribbons at a heating rate of 20 K min^{-1} is reproduced in Fig. 1. The glass was found to crystallize in two stages: first, a slight precipitation of a nickel-phase was detected. Also, some lines of a $Cr_3Ni_5Si_2$ phase were identified. After completion of the second stage, nickel and Ni_3Si-type phases are found. The peak temperatures of both crystallization stages were 747 and 821 K. Temperatures of isothermal anneals were selected in the range 697 to 775 K after a few trial runs. Anneals at higher temperatures could not be carried out because of the difficulty usually encountered of the incubation time falling short of the instrument transient time. At lower temperatures, because of the slow transformation rates, the exotherms tended to flatten out. In the temperature range of the investigation used, the baseline became linear after the end of the instrument transient/completion of the previous crystallization stage, and well-defined isothermal exotherms could be obtained. The start of the transformation was taken as the instant at which the baseline first deviated from linearity.

Because the crystallization occurs by nucleation and growth, kinetics on isothermal annealing should be described by the Johnson–Mehl–Avrami equation: $x(t) = 1 - \exp(-bt^n)$ where $x(t)$ is the fraction transformed at time t, b is a rate constant which depends on both the nucleation rate and the growth rate and n is the Avrami exponent that depends on the mechanisms of the crystallization. Plots of x against t at different annealing temperatures for the two crystallization stages yielded the sigmoidal curves shown in Fig. 2. Each data point is derived from the integrated intensity under the isothermal curve at that temperature as explained in Section 2.

Fig. 3 shows the ln–ln plots of $-\ln(1-x)$ against t. For the first exotherm the experimental points display a double-slope behaviour, whereas for the second exotherm the points can be roughly fitted to a straight line. Values obtained for the mean Avrami exponent are, approximately, 2.5 for the early straight line and 1.5 for the late straight line of the first crystallization stage and a value close to 4.0 is found for the second stage.

Unambiguous interpretation of the experimental crystallization kinetics is difficult when microscopic observations are not available, because of the possibility of several kinds of sites with different nucleation rates and modes of growth. However, it may be helpful to examine the results in the light of an approximate model [8]. Here, it is assumed that $n = a + bp$, where a accounts for the nucleation rate and varies from

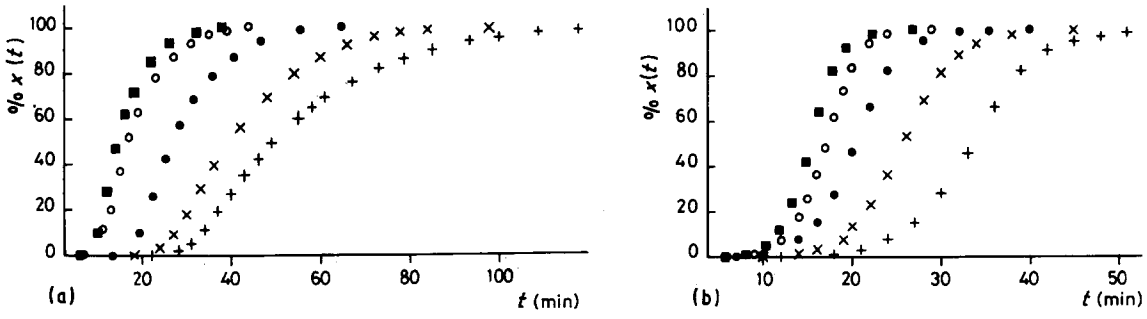

Figure 2 Crystallized fraction plotted against time for (a) the first and (b) the second crystallization stage. (a) (■) 710 K, (○) 708 K, (●) 703 K, (×) 700 K, (+) 697 K. (b) (■) 775 K, (○) 773 K, (●) 770 K, (×) 767 K, (+) 762 K.

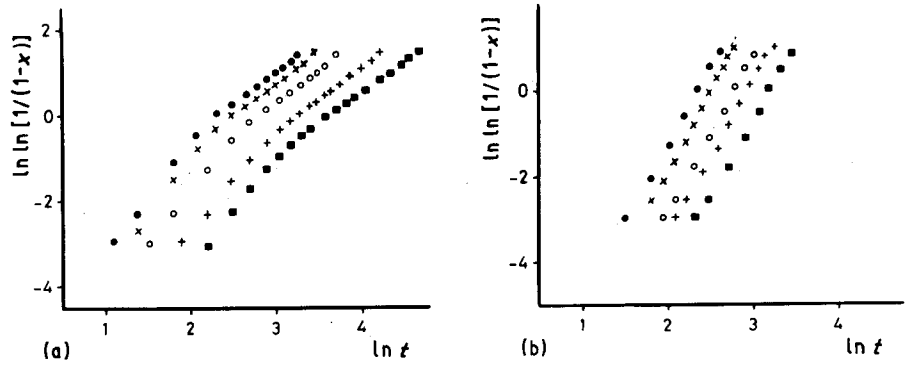

Figure 3 Plots of the JMA equation for different isothermal runs: (a) first and (b) second. (a) (●) 710 K, (×) 708 K, (○) 703 K, (+) 700 K, (■) 697 K. (b) (●) 775 K, (×) 773 K, (○) 770 K, (+) 767 K, (■) 762 K.

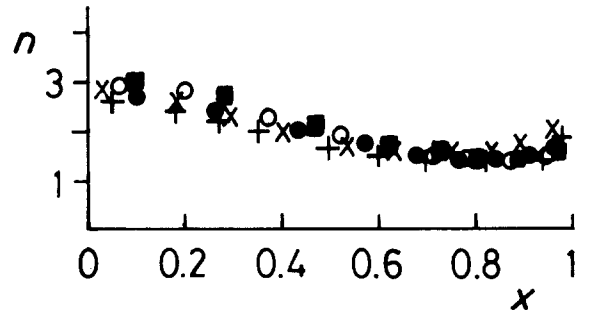

Figure 4 The modified Avrami plot (n_{loc}–x) for the first crystallization stage. For key, see Fig. 3a.

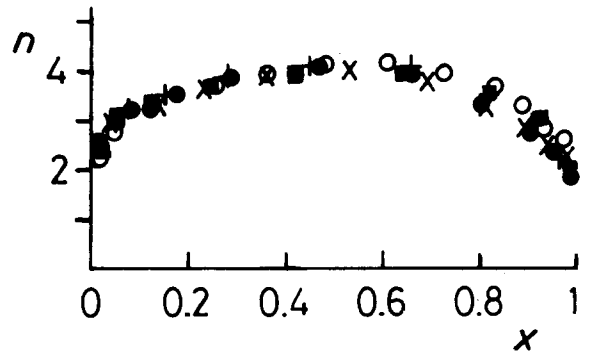

Figure 5 The $n_{loc}(x)$ plot for the second crystallization stage. For key, see Fig. 3b.

zero (for quenched-in nuclei) to 1 (for a constant nucleation rate), b defines the dimensionality of the growth (b = 1, 2, or 3), p has the value 1 for interfacial control of growth (assumed linear in time), and p = 0.5 for diffusion-controlled growth.

Thus, the value 2.5 obtained for the early straight line of the first exotherm points to three-dimensional diffusion-controlled growth with a constant nucleation rate. The same value, n = 2.5, was found for the Avrami index of the first crystallization stage of other analogous nickel-based alloys previously reported [9, 10] and should correspond to the precipitation of nickel particles in the amorphous matrix. In this case, the mean Avrami exponent decreases to 1.5 for the late straight line of the first exotherm and this value should correspond to a zero nucleation rate. For the second crystallization stage the value n = 4.0 suggests interface-controlled growth with constant nucleation rate. This value of the Avrami index is also obtained in other nickel-based alloys [10].

The activation energy for the overall crystallization process can be obtained from the temperature dependence of the rate constant [11]. A straight line fit of $\ln b$ against $1/T$, as required for the Arrhenius relation, is reasonably well achieved for the second exotherm and the slope yields a value of 319 kJ mol^{-1} (3.3 eV at^{-1}) for the activation energy of the second crystallization stage. This activation energy obtained from isothermal kinetics is slightly lower than that obtained by Kissinger's method for the non-isothermal process (335 kJ mol^{-1}). For the first exotherm this approach is not appropriate because of the double-slope behaviour of the log–log plot cited above. Activation energy, in this case, can be obtained for each x range from a plot of $1/T$ against $\ln t(x)$, where $t(x)$ is the time corresponding to a value x of the transformed fraction, from the sigmoidal curves $x(t)$ at various temperatures, T. So, for values x = 0.2, 0.5 and 0.8, the activation energy is 359, 382 and 397 kJ mol^{-1}, respectively. All these values are lower than that obtained by the Kissinger's method (419 kJ mol^{-1}).

It is clear that the experimentally determined Avrami index could be expected to be a constant only in some limiting cases. In reality, either the growth morphology or the nucleation rate, or both, may change as the crystallization process proceeds. The variation of n with the volume fraction transformed was analysed by plotting the time derivative of ln [− ln (1 − x)] against volume fraction transformed at each temperature for the two crystallization stages. Fig. 4 illustrates the variation of the modified Avrami index, n, with (x) during the first crystallization stage. As observed, the variation with the crystallized fraction is similar for all the isothermal anneals: the plots collapse in a single curve. Initially, at the beginning of crystallization, n is close to 3.0, then it decays uniformly, as the crystallized fraction increases, to reach a value close to 1.5 and finally, for $x > 0.85$, a slight increase of n_{loc} is observed. Unambiguous interpretation cannot be given without detailed TEM studies; however, the observed decrease in the n_{loc} value should be attributed to a non-steady nucleation with an increasing rate ($n_{loc} > 2.5$) initially, and a decreasing rate ($1.5 < n_{loc} < 2.5$) when the crystallized fraction increases.

Fig. 5 shows the behaviour of the modified Avrami coefficient for the second crystallization stage. As observed, the variation of n_{loc} with the crystallized fraction is similar for all the isothermal crystallization temperatures: n_{loc} increases in the range $0 < x < 0.3$ to

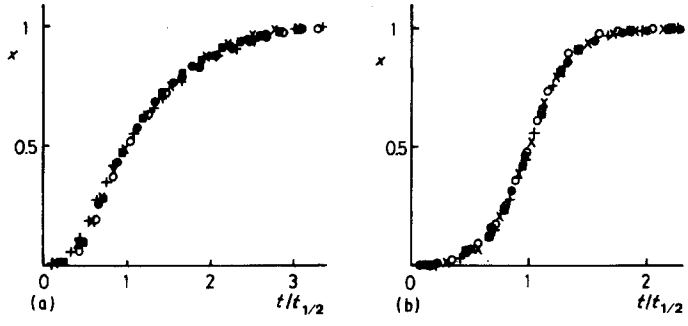

Figure 6 Time-scaled curves of crystallized fraction: (a) first stage, (b) second stage.

reach a value of 4.0, and decreases monotonically for crystallized fractions $x > 0.8$. The initial increase in n_{loc} should be assigned to a non-steady homogeneous nucleation with interface-controlled growth and then, for $0.3 < x < 0.8$, crystallization progresses dominated by a constant nucleation rate. Finally, the decrease in the n_{loc} value for $x > 0.8$ should be caused by a decreasing nucleation rate and also the three-dimensional growth should be affected by impingement.

To analyse time-scaling properties of the isothermal crystallization kinetics, for each isotherm, the time $t_{1/2}$ for which $x = 0.5$ can be found experimentally and the time scale of each isotherm can be redefined as $t/t_{1/2}$ [12]. In this way, all the time-scaled isotherms relative to each transformation stage lie on a single curve, as shown in Fig. 6, demonstrating that the transformation kinetics obeys a time-scaling law. Scaling properties of some metallic glasses have been recently reported [12–14].

4. Conclusions

The results of the crystallization kinetics are consistent with a three-dimensional diffusion-controlled growth primary precipitation of nickel particles in the first stage and a polymorphic interface-controlled crystallization in the second stage. The variation of n_{loc} with the crystallized volume fraction is independent of the temperature of the isothermal anneals, indicating that the process depends only on the volume fraction transformed. The features of the n_{loc} against x plots enable the observation of subtle effects in the transformation, even when interpretation of the plots is not straightforward. Finally, it is demonstrated that the transformation kinetics obeys a time-scaling law.

Acknowledgements

This work was supported by the CICYT of the Spanish Government (Project MAT88-301) and by the "Junta de Andalucia".

References

1. F. E. LUBORSKY (ed), "Amorphous Metallic Alloys", Butterworths Monographs in Materials (Butterworths, London, 1983).
2. T. R. ANATHARAMAN (ed), "Metallic Glasses, Production, Properties and Applications" (Trans. Tech., Aedermannsderg, 1984).
3. A. CALKA and A. P. RADLINSKI, *Mater. Sci. Engng.* **97** (1988) 241.
4. H. MIRANDA, C. F. CONDE, A. CONDE and R. MARQUEZ, *Mater. Lett.* **4** (1986) 442.
5. C. F. CONDE, H. MIRANDA, A. CONDE and R. MARQUEZ, *J. Mater. Sci. Lett.* **6** (1987) 257.
6. M. A. GIBSON and G. W. DELAMORE, *J. Mater. Sci.* **22** (1987) 4550.
7. M. MILLAN and A. CONDE, *Mater. Lett.* **8** (1989) 271.
8. V. R. V. RAMANAN and G. FISH, *J. Appl. Phys.* **53** (1982) 2273.
9. C. F. CONDE, H. MIRANDA, A CONDE and R. MARQUEZ *J. Mater. Sci.* **24** (1989) 139.
10. H. MIRANDA, C. F. CONDE and A. CONDE, **8** (1989) 400.
11. J. W. CHRISTIAN, "The Theory of Transformations in Metals and Alloys", 2nd Edn (Pergamon, Oxford, 1981) p. 51.
12. C. F. CONDE, H. MIRANDA and A. CONDE, *J. Mater. Sci.* **24** (1989) 1862.
13. Y. WOLFUS, Y. YESHURUN, I. FELLNER and J. WOLNY, *Solid State Commun.* **61** (1987) 519.
14. A. ROIG, J. S. MUÑOZ, M. B. SALOMON and K. V. RAO, *Appl. Phys.* **61** (1987) 3647.

Received 31 July 1989
and accepted 6 February 1990